

DELFT UNIVERSITY OF TECHNOLOGY

REPORT 17-10

MATHEMATICAL MODELING OF COMBUSTION REACTIONS IN  
TURBULENT FLOW OF ANODE BAKING PROCESS

P.A. NAKATE

ISSN 1389-6520

Reports of the Delft Institute of Applied Mathematics

Delft 2017

# 1 Introduction

Anode baking process is the most important process in the aluminium industry. A more uniform temperature distribution is desired inside the anode during the heating process. Generally, anodes are baked in ring furnaces. There are two types of ring furnaces, open ring furnace or closed ring furnace. In the present industry, open ring furnace is used to bake the anodes. A good anode baking process needs to achieve following goals [1].

- Anodes of uniform quality
- Soot free combustion
- Lowest possible NO<sub>x</sub> generation
- maintenance cost
- High furnace life time

The current practices fail to meet these goals to a complete extend. Therefore, research study is required in order to understand the physics occurring in the process so as to meet these goals by improving or making necessary changes. Mathematical modeling in this respect can be of importance since it defines the system based on the physical theories and helps in predicting the behaviour of different parameters with strong evidence of physics.

Anode baking process is explained in the next section followed by the objectives and approach of this work.

## Understanding of the overall anode baking process

The main objectives of the anode baking process are following:

- To make sure that the mechanical properties of the matter are homogeneous
- To make anode conductive
- To minimize anode reactivity during electrolysis

The typical composition of a prebaked anode, which is referred as Green anode, is 85% of dry matter and 15% of pitch. This pitch has 33% of volatile matter which are released during anode baking process and the remainder part of pitch is converted into binding coke. Figure 1 illustrates the transformation of anode material during baking process.

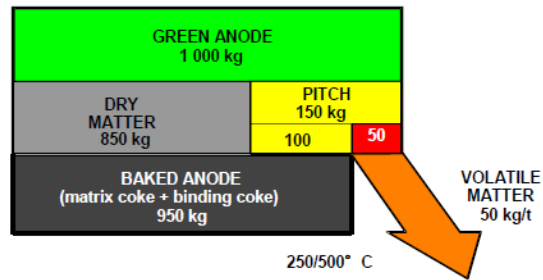


Figure 1: Transformation of anode material during anode baking process

In order to bake the anodes open ring furnaces are used. These furnaces involve alternate arrangement of flue walls and pits as shown in Figure 2. Gas flows through the flue walls to generate heat by combustion process in certain sections of the furnace. Whereas, green anodes are placed in the pits.

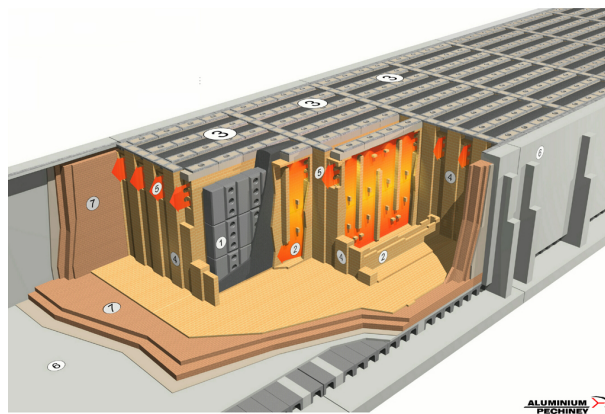


Figure 2: Overall geometry of anode baking furnace

There are various zones involved in the furnace that define the exchange of heat occurring in that section. Figure 3 gives the idea of these various zones. As shown in the figure, anodes first go through the preheating zone. Here, hot fumes that are coming from the heating section exchanges heat with cold anodes and as a result, volatiles are released by the anodes. In the preheating section, combustion of these volatiles take place which also contributes to the generated heat. Partially heated anodes are then shifted to heating section. It should be noted that anodes are not moving from one section to another. But heating and blowing ramps are moved in such a way that the anodes undergo through all the zones sequentially. In the heating zone, burners introduce natural gas which combines with gas flowing through the flue

wall. Here, combustion of gases occur and large amount of heat is generated. Heating zone is followed by the blowing zone. In this zone, heat is exchanged from hot anodes to cold air and therefore, anodes are partially cooled. In the subsequent zone, i.e., in the cooling zone, external cooling facilities are applied so as to cool down the anodes to a desired temperature. Air is blown in the blowing zone and is taken out from the exhaust ramp. Therefore, pressure in the blowing zone is more than atmospheric pressure in blowing zone. Whereas, it is lesser in preheating zone. Therefore, there is a point in the furnace where pressure is exactly equal to atmospheric pressure. This point is referred as zero point measurement.

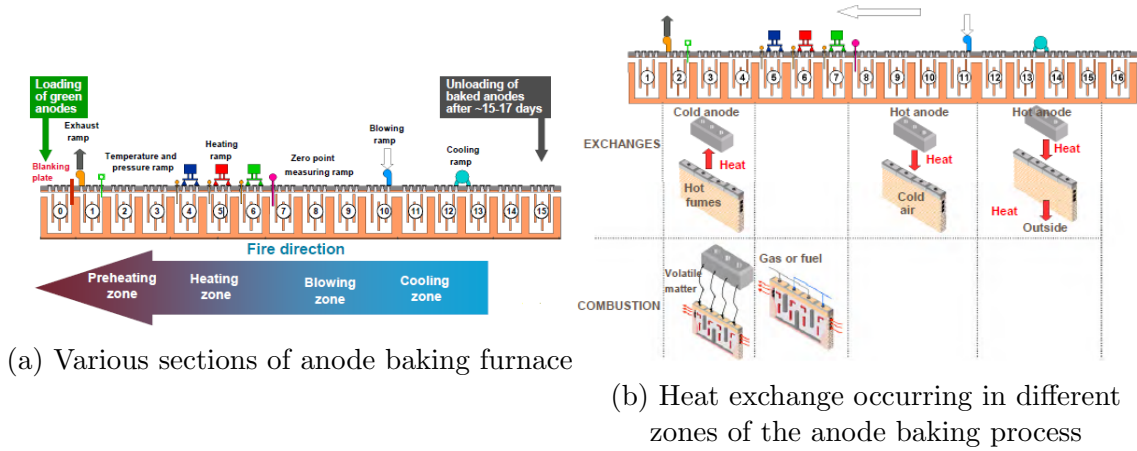


Figure 3: Geometry of the overall furnace in the direction of fluid flow

## Objectives of the project

In the present work, focus is given to reduce NO<sub>x</sub> from emissions. NO<sub>x</sub> generation in the furnace is mainly due to high temperature around the burner. At present, knowledge of temperature distribution around the burner is lacking. Therefore, this assignment focuses on the modelling of combustion process to know the temperature distribution around the burner. The process of combustion is accompanied by the turbulent flow of the gas. Therefore, modelling of turbulent flow is also required for the complete understanding of the process.

In order to develop temperature distribution around the burner, following nascent models in COMSOL Multiphysics software are developed in the present work.

- Turbulent flow model in the section of the furnace
- Reacting turbulent flow near the domain of the fuel inlet

- Addition of heat effects (such as heat generation due to the combustion process, radiation transfer in the domain and heat conduction through the walls) to the reacting flow model

This report focuses on the background theory, development and results of these models followed by the recommendations for future work.

## 2 Model

### 2.1 Introduction

Anode baking process includes occurrence of multiple physical phenomena which need to be understood before diving into its mathematical model. The physics behind these phenomena can be complicated and may demand simplification while translating into a model. This is also necessary in order to have rational computational costs. However, these simplifications should be such that they retain the resemblance with the physical phenomena occurring in the actual application. In order to attain this, physical phenomena is converted into mathematical equations. These mathematical equations might be complex and may need several simplifications to arrive at the desired solution.

Fluid flow is of prime importance in combustion process occurring in the anode baking furnace. The geometry of the furnace is such that the viscous forces dominate over inertial forces. This imply that the flow in the furnace is highly turbulent. Therefore, the two major phenomena which govern the anode baking process are turbulence and combustion. These two phenomena are strongly dependent on each other. Turbulence produces eddies which facilitates the higher mixing in the system. Higher mixing leads to efficient chemical reaction, i.e., combustion reaction. Combustion process is accompanied by the release of heat. Increase in enthalpy creates more turbulence due to buoyancy effects. Therefore, the two physical phenomena are highly dependent [2]. Turbulence is accompanied by the generation of eddies. As a result of this, mass, heat and momentum are efficiently exchanged between different species in the system [3]. In other words, eddies propel higher mixing of chemical species which lead to efficient chemical reaction in the system. These chemical reactions occurring in the anode baking furnace release significant heat of reaction. Therefore, the enthalpy in the furnace is increased which drive eddies to produce more turbulence. This strong dependence of the two phenomena needs to be accounted while modeling the combustion process via the coupling of different physics.

Turbulence is attributed by flow and therefore can be described by the momentum equation. Whereas, combustion process can be defined by the balance of chemical

species and enthalpy change in the system. Therefore, the overall anode baking process can be mathematically modeled by following four major balance equations.

1. Mass conservation (Continuity equation)
2. Momentum balance
3. Energy balance
4. Balance of chemical species

In the following section, the four major balance equations are elaborated.

## 2.2 Governing Equations

### 2.2.1 Continuity- Mass conservation

Continuity equation is based on the law of conservation of mass which states that "in an isolated system, mass can neither be created nor destroyed by chemical reactions or physical transformations" [4] and is given by equation 1 [3, 2].

$$\frac{\partial \rho}{\partial t} + \frac{\partial(\rho u_i)}{\partial x_i} = 0 \quad (1)$$

where,  $\rho$  is the density of fluid,  $t$  is time and  $u_i$  is the velocity vector in  $i$  direction. The first term of the equation represents the accumulation of mass with respect to time in a control volume whereas, the second term represents the net flux of mass through the control volume. In the combustion process, density is variable as the fluid in the process is in gaseous state and therefore, density strongly depends on pressure, temperature and chemical species [3]. Density is calculated by assuming gas in the furnace as ideal gas. Moreover, flow in the simulations performed in the present work are assumed to be in the steady state. Therefore, equation 1 can be simplified to following equation 2.

$$\frac{\partial(\rho u_i)}{\partial x_i} = 0 \quad (2)$$

In most of the simulations, continuity equation is solved along with the momentum equation (explained in the next section) as the velocity is the characteristics of the flow.

### 2.2.2 Momentum balance equation- Navier-Stokes equation

Momentum is used to quantify flow of the fluid and is defined as the product of mass and velocity. Momentum balance equation is governed by the law of conservation of momentum. This law is based on the Newtons laws of motion and states that the total momentum in a closed system is constant. Navier-Stokes equation is the particular form of momentum conservation equation and is given by equation 3.

$$\frac{\partial(\rho u_i)}{\partial t} + \frac{\partial(\rho u_i u_j)}{\partial x_j} = \frac{\partial p}{\partial x_i} + \frac{\partial \tau_{ij}}{\partial x_j} + F_i \quad (3)$$

where,  $\rho$  is the density,  $u_i$  and  $u_j$  are the velocity vectors in  $i$  and  $j$  direction, respectively,  $t$  is time,  $p$  is pressure,  $\tau_{ij}$  is the viscous stress tensor and  $F_i$  is the external body force vector. The first term of the equation represents the accumulation of momentum with respect to time in the control volume, the second term represents the net flux of momentum through the control volume, the third term is the pressure and viscous stresses applied to the control volume and the fourth term represents the external body forces (such as gravity) acting on the control volume.

The fluid in the furnace is assumed to be a Newtonian fluid. Therefore, according to Stokes's assumption the viscous stress tensor can further be elaborated as given in equation 4.

$$\tau_{ij} = \mu \left( \frac{\partial u_i}{\partial x_j} + \frac{\partial u_j}{\partial x_i} + \frac{2}{3} \frac{\partial u_k}{\partial x_k} \delta_{ij} \right) \quad (4)$$

where,  $\mu$  is dynamic viscosity. Substituting equation 4 in equation 3 gives a complete momentum balance equation. Therefore, complete momentum balance equation is as shown in equation 5.

$$\frac{\partial(\rho u_i)}{\partial t} + \frac{\partial(\rho u_i u_j)}{\partial x_j} = \frac{\partial \left( p + \mu \left( \frac{\partial u_i}{\partial x_j} + \frac{\partial u_j}{\partial x_i} + \frac{2}{3} \frac{\partial u_k}{\partial x_k} \delta_{ij} \right) \right)}{\partial x_j} + F_i \quad (5)$$

As mentioned earlier, flow in the anode baking furnace is highly turbulent due to dominating viscous forces. Generalized Navier-Stokes equation 5 needs several modifications in order to define turbulent flow. This is further elaborated in section 10.

### 2.2.3 Chemical species balance

Chemical species balance is one of the major equation concerning reacting flows and is based on the conservation of mass. "The number of atoms of any given element does not change in any reaction (assuming that it is not a nuclear reaction)" [5]. Therefore, every chemical species can be balanced in a given control volume and can be related by equation 6 [3].

$$\frac{\partial(\rho Y_s)}{\partial t} + \frac{\partial(\rho u_j Y_s)}{\partial x_j} = \frac{\partial(\rho J_s)}{\partial x_j} + \dot{\omega}_s \quad s = 1, 2, \dots, m \quad (6)$$

where,  $Y$  is the mass fraction of species  $s$  and  $J_s$  stands for diffusive flux of species  $s$ . The first term of the equation represents the accumulation of species  $s$  in the control volume, second term represents the convective flux, third term represents the diffusive flux and fourth term represents the rate of generation/consumption of species  $s$  in the control volume. Fick's law of diffusion is used to further elaborate the diffusive flux term in the equation. By substituting Fick's law of diffusivity in equation 6, complete chemical species balance equation can be obtained as:

$$\frac{\partial(\rho Y_s)}{\partial t} + \frac{\partial(\rho u_j Y_s)}{\partial x_j} = \frac{\partial([\rho D_s \frac{\partial Y_s}{\partial x_j}])}{\partial x_j} + \dot{\omega}_s \quad s = 1, 2, \dots, m \quad (7)$$

The rate of generation/consumption of any chemical species is obtained by the knowledge of chemical reaction rate. This rate is based on the reaction rate law which is a combination of rate constant and concentration of species to the power of its stoichiometric coefficient. The rate constant appearing in the rate law is obtained from the Arrhenius rate law which related rate constant to the activation energy and temperature. Moreover, reaction rate also depends on the contact between different species which is governed by the mixing. In the present furnace, reaction is occurring in the turbulent flow of gases. Reaction rate might also depend on the turbulence in the system which induces mixing of different species. Therefore, reaction rate highly depends on whether the system is reaction time limited or mixing limited. In most of the furnaces in which flow is turbulent, mixing is slower than the reaction time. Different reaction models are available which can define such behaviour in the furnace. One such model is elaborated in section 2.4.3.

#### 2.2.4 Energy balance

Another important balance in combustion process of anode baking is the energy balance equation. Energy balance is based on the first law of thermodynamics which states that energy can neither be created nor destroyed and can only be modified from one form to another. Equation 8 represent the simple form of energy balance in terms of the enthalpy.

$$\frac{\partial(\rho h)}{\partial t} + \frac{\partial(\rho u_i h)}{\partial x_i} = \frac{\partial q_d}{\partial x_i} + \dot{h}_s \quad (8)$$

where,  $q_d$  is the diffusive transfer of enthalpy and  $\dot{h}_s$  is the rate of generation/dissipation of enthalpy. The first term of the equation represents the accumulation of enthalpy



with respect to time in the given control volume, second term represents the convective enthalpy flux, third term represents the diffusive enthalpy flux and fourth term represents the generation/consumption of enthalpy.

Enthalpy of a mixture is the summation of the product of enthalpy of the individual species and its mole fraction. Enthalpy of the individual species are calculated from the specific heat capacity of the chemical species. In the present work, specific heat capacity of the chemical species, which are function of temperature, are estimated from the interpolation function.

Diffusive flux of enthalpy in the combustion process can either be due to the gradient of temperature in the furnace or due to transfer of enthalpy due to species diffusion. In the present work, diffusive flux due to enthalpy transfer is assumed to be negligible. Diffusive flux due to temperature gradient, i.e., conduction can be defined by Fourier's law of conduction. Combustion reaction is accompanied by the release of heat. Therefore, change in enthalpy is observed as a result of the reaction. Radiation is another heat transfer media which is dominating in combustion process. The fourth term of the equation may consist of several terms which change enthalpy during combustion process. Some of these sources are chemical reaction, viscous heating, pressure work and radiation. In the present case, only chemical reaction and radiation are assumed to be significant. Details of the heat released by chemical reaction and radiation model are explained in section 3.3.3 and 2.4.4. Implementing all the assumptions and expression for diffusive flux, complete energy equation is as shown by equation 9.

$$\frac{\partial(\rho C_p T)}{\partial t} + \frac{\partial(\rho u_i C_p T)}{\partial x_i} = \frac{\partial(-k \frac{\partial T}{\partial x_i})}{\partial x_i} + \dot{h}_s \quad (9)$$

## 2.3 Boundary conditions

In order to solve above governing differential equations, following boundary conditions are needed.

### 2.3.1 Velocity

Velocity at inlet of air and fuel are specified based on the available data. Wall functions are used to define velocity at the wall. The equation used in wall function is described in appendix A.1 [3]. Direction of velocity at the outlet is defined such that it is normal to the outlet cross section. Boundary conditions for average turbulent kinetic energy and turbulence dissipation rate is specified as zero at the inlet and defined at the wall according to wall function given in appendix A.1.

### 2.3.2 Pressure

Pressure at the outlet is specified based on the available data.

### 2.3.3 Mass fraction

Mass fraction of all the chemical species are specified at the inlet of air and fuel as per the available information. Mass flux normal to the wall is defined as zero.

### 2.3.4 Temperature

Temperature at the inlet of air and fuel, at the wall in contact with external environment, wall in contact with fluid domain are specified as per the available information. Heat flux in thermally insulated walls is defined as zero.

### 2.3.5 Radiation intensity

Boundary condition for radiation intensity is defined by the Marshak boundary condition as given in appendix A.2.

## 2.4 Physical models

All the physical phenomena occurring in the anode baking process can be translated into mathematical equations as described in the previous section. However, in order to make these mathematical equations solvable, they need to be simplified by making certain assumptions. Such simplified mathematical expressions are the basis of any physical model. In the present section, physical models that are used for building a complete combustion model of anode baking process are described. These models are extensively used in turbulent combustion modeling [6, 7, 8]

### 2.4.1 Reynolds-averaged Navier-Stokes equation (RANS)

Turbulence is the most complicated physical phenomena in anode baking process, as it deals with large amount of fluctuations. Solving mathematical expressions that deal with these fluctuations might be complex. Moreover, in most of the industry processes, time averaged properties can provide significant desired information. Therefore, in this respect, RANS equation can be of importance. In this equation, spatial variation in physical properties such as density, viscosity etc. are averaged using Favre average statistical approach. Turbulence can be simplified by decomposing velocity into mean part and fluctuating part. RANS, as the name suggests, take the time average of Navier-Stokes equation resulting in the mean flow equation. Equation 10 represents this RANS equation.

$$\frac{\partial(\bar{\rho}\tilde{u}_i)}{\partial t} + \frac{\partial(\bar{\rho}\tilde{u}_i\tilde{u}_j)}{\partial x_j} = -\frac{\partial\bar{p}}{\partial x_i} + \frac{\partial[\mu(\frac{\partial\tilde{u}_i}{\partial x_j} + \frac{\partial\tilde{u}_j}{\partial x_i})]}{\partial x_j} - \frac{\partial(\bar{\rho}\widetilde{u'_i u'_j})}{\partial x_j} \quad (10)$$

In this equation, first term represents the accumulation of average momentum in a control volume, second term represents the net average convective flux through the control volume, third term represents the average pressure gradient, fourth term represents the average gradient of viscous stresses while the last term is the nonlinear term which quantifies velocity fluctuations and is referred as "Reynolds stress". Reynolds stress increases as the mean rate of deformation increases [3]. Therefore, Boussinesq proposed an equation, given by equation 11, which relates Reynolds stress with mean rate of deformation.

$$\bar{\rho}\widetilde{u'_i u'_j} = \mu_t(\frac{\partial\tilde{u}_i}{\partial x_j} + \frac{\partial\tilde{u}_j}{\partial x_i}) - \frac{2}{3}\rho k\delta_{ij} \quad (11)$$

where,  $\mu_t$  is the turbulent viscosity,  $k$  is the turbulent kinetic energy per unit mass and  $\delta_{ij}$  is the Kronecker delta which ensures that the formula gives normal Reynolds stresses. Several models are available to define turbulent viscosity and average kinetic energy. In the present work,  $k - \epsilon$  model is used to elaborate these quantities.

#### 2.4.2

$k - \epsilon$  model

$k - \epsilon$  model focuses on calculating turbulent kinetic energy and turbulent energy dissipation rate. Two scalar transport equations, given by equation 12 and 13, are simultaneously solved with RANS equation to quantify instantaneous kinetic energy.

$$\frac{\partial(\bar{\rho}\tilde{k})}{\partial t} + \frac{\partial(\bar{\rho}\tilde{u}_j\tilde{k})}{\partial x_j} = \frac{\partial[\mu_{eff}^\epsilon \frac{\partial\tilde{k}}{\partial x_j}]}{\partial x_j} + \mu_t \frac{\partial\tilde{u}_i}{\partial x_j} [\frac{\partial\tilde{u}_i}{\partial x_j} + \frac{\partial\tilde{u}_j}{\partial x_i}] - \bar{\rho}\tilde{\epsilon} \quad (12)$$

$$\frac{\partial(\bar{\rho}\tilde{\epsilon})}{\partial t} + \frac{\partial(\bar{\rho}\tilde{u}_j\tilde{\epsilon})}{\partial x_j} = \frac{\partial[\mu_{eff}^\epsilon \frac{\partial\tilde{\epsilon}}{\partial x_j}]}{\partial x_j} + C_{\epsilon 1} \frac{\tilde{\epsilon}}{\tilde{k}} \mu_t \frac{\partial\tilde{u}_i}{\partial x_j} [\frac{\partial\tilde{u}_i}{\partial x_j} + \frac{\partial\tilde{u}_j}{\partial x_i}] - C_{\epsilon 2} \bar{\rho} \frac{\tilde{\epsilon}^2}{\tilde{k}} \quad (13)$$

where,  $\mu_{eff}^\epsilon$  is the combination of dynamic and turbulent viscosity and is given by equation 14.

$$\mu_{eff}^\epsilon = \mu + \frac{\mu_t}{\sigma_\epsilon} \quad (14)$$

where,  $\sigma_\epsilon$  is Prandtl number turbulent energy dissipation rate.  $\mu_t$  is defined as a constant given by equation 15.

$$\mu_t = C_\mu \frac{\tilde{k}^2}{\tilde{\epsilon}} \quad (15)$$

The values of constants used in all the above equations are:

$$\sigma_k = 1, \sigma_\epsilon = 1.3, C_\mu = 0.09, C_{\epsilon 1} = 1.44, C_{\epsilon 2} = 1.92$$

### 2.4.3 Eddy-dissipation model

Chemical reaction is another important physical phenomena occurring in combustion process. The rate of generation or consumption of any chemical species is governed by the rate of chemical reaction. Heat of the reaction in the process is also controlled by the rate of reaction. Therefore, establishing model for calculating rate of reaction is important. In the present work, it is assumed that the combustion process is non-premixed, i.e., fuel and air are not mixed before the combustion process. Therefore, rate of reaction can either be controlled by turbulent mixing or reaction time. There are several models to quantify the rate of such combustion reactions occurring in turbulent flow. Here, eddy-dissipation model has been used [9].

Eddy-dissipation model assumes that the rate of reaction is infinitely fast. Moreover, turbulent mixing time is the dominating time scale [10]. Following equation represents the eddy dissipation model.

$$R_i = \nu_i M_i \rho \frac{\alpha}{\tau_T} \beta \sum_p \left( \frac{w_p}{\nu_p M_p} \right) \quad (16)$$

Here,  $R_i$  is the reaction rate of species  $i$ ,  $\nu_i$  is the stoichiometric coefficient of  $i$ ,  $M_i$  is the molecular weight of component  $i$ ,  $\rho$  is the density,  $\tau_T$  is the turbulent mixing time scale,  $w_p$  is weight fraction of product.

Eddy-dissipation is a simple and robust reaction rate model that connects reaction rate with turbulent mixing. However, this model has certain disadvantages such as it overestimates the fuel consumption [10].

### 2.4.4 P1 Radiation model

Radiation is a significant heat transfer mechanism when the temperature of the body matter is more than 1000 K. In order to calculate the complicated total radiation intensity term from radiative transfer equation, P1 approximation method is used [11]. Following two equations define the radiative heat flux using P1 approximation method [2, 12, 13].

$$q = -\frac{1}{3\kappa_\lambda} \nabla G \quad (17)$$

Therefore, simplified radiative heat transfer equation is as given by equation 18 [12].

$$\nabla \cdot \left( \frac{1}{3\kappa} \nabla G \right) = \kappa G - 4\kappa\sigma T^4 \quad (18)$$

This radiation model assumes that the radiation intensity is isotropic at a given space. Though this assumption does not completely hold true in the present case, P1 approximation model is preferred due to its simplicity and low computational cost. However, COMSOL Multiphysics allows implementing other radiation models such as DOM, Roseland as well.

### 3 Implementation in COMSOL

In the previous chapter, all physical phenomena that are involved in the anode baking combustion process are described along with the simplified models that are used to define associated physics. Present chapter focuses on the approach of building a combined model which simultaneously deals with different physics of the process with the help of COMSOL Multiphysics software.

COMSOL has various modules for dealing with different physics. In the present work, simple models with individual physics assuming negligible effects of other physical phenomena are built as a first step. The overall model is split into 3 parts for the initial study. These three parts are:

- Turbulent flow
- Reacting turbulent flow
- Combined Model of reacting flow and heat release

In this chapter, these 3 parts of the initial study are described followed by the combined model of the three physics.

#### 3.1 Turbulent flow

As a first step, turbulent flow of air in one section of the furnace is modeled. In the present section, this turbulent flow model of air is described.

##### 3.1.1 Geometry

A complete one section of the furnace is chosen as the geometry for modeling turbulent flow as shown in Figure 4. As can be seen in the Figure, section has three baffles, and number of tie-bricks in order to regulate the flow. The grey areas represents the

domain of fluid flow. The purpose of this model is to gain complete understanding of the nature of the air flow inside the furnace. Therefore, fuel is not introduced in this model.

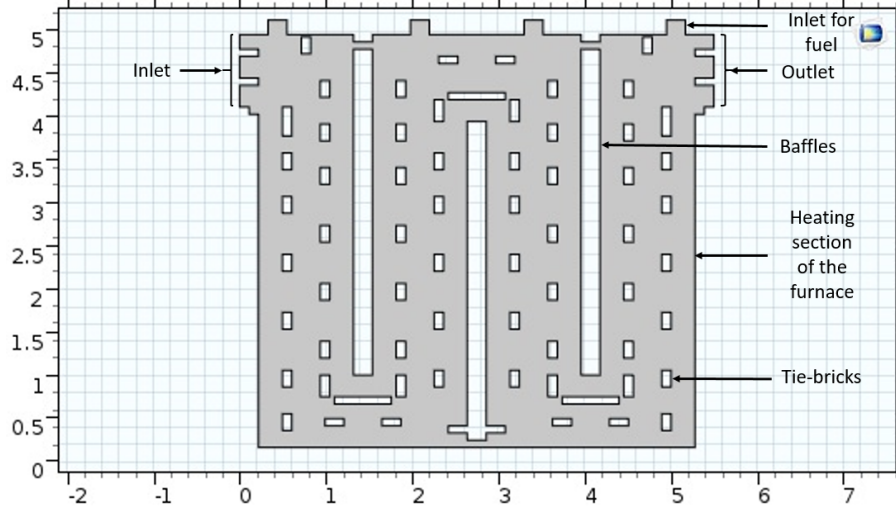


Figure 4: Geometry for the turbulent flow model

### 3.1.2 Physics

COMSOL Multiphysics provides various physics modules from which turbulent flow is selected from the single phase flow of "Fluid flow" module. RANS is selected as the turbulence model type and  $k - \epsilon$  model is used to define the turbulent viscosity and average kinetic energy parameters for RANS equation. Details of these models are described in section 10.

### 3.1.3 Boundary conditions

Table 1 shows the required boundary conditions for each of the dependent variable from the number of equations solved for the current model.

Table 2 presents the actual values of initial and boundary conditions for the aforementioned variables.

Here, wf is the wall function and is used to describe boundary conditions at wall as described in appendix A.1.

### 3.1.4 Mesh

Fine triangular mesh is used to divide the entire domain into short sub-domains.

Table 1: Number of boundary conditions required for the participating dependent variables

Variable	Required boundary conditions	Boundary condition
Velocity	2	Inlet, Wall
Pressure	1	Outlet
Turbulent kinetic energy	2	Inlet, Wall
Turbulent dissipation rate	2	Inlet, Wall

Table 2: Initial and boundary conditions

	Velocity ( $m/s$ )	Pressure ( $atm$ )	$k$ ( $m^2/s^2$ )	$\epsilon$ ( $m^2/s^3$ )
Initial conditions	0	0	0	0
Inlet	1.3	-	0	0
Wall	0	-	wf	wf
Outlet	-	1	-	-

### 3.1.5 Study

Default linear discretization scheme is used to discretize the components of the equations. In order to solve the equations, PARDISO direct numerical solver is used. Segregated step approach is used to solve the different variables.

### 3.1.6 Results

Surface plots of velocity and turbulent viscosity for the turbulent flow model are as shown in Figure 5.

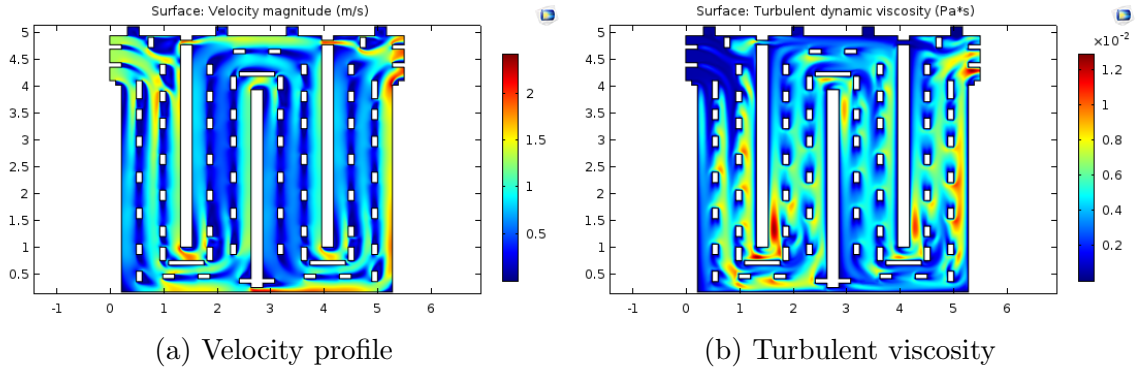


Figure 5: Model results of turbulent flow of air

Figure 5a shows that the velocity is regulated by the baffles and tie-bricks and there-

fore, the velocity distribution would be sensible with respect to their position. As can be expected, velocity through the small channel at the top is quite high due to smaller cross section. Moreover, the velocity profiles at inlet and outlet confirm that the continuity equation is correctly implemented. The velocity distribution in the model can not exactly validated because of the unavailability of the velocity distribution plots. However, comparison with the earlier study (Figure 14 from appendix B.1) of the similar furnace model shows that the flow patterns are aligned for the present and earlier study.

Turbulent viscosity can be used to characterize the turbulence in the furnace. Though turbulent viscosity is not a physical concept, it can be used to understand the intensity of turbulent stresses generated by eddies. The tie-bricks in the furnace induce turbulence resulting into turbulent stresses and therefore, higher turbulent viscosity is observed near these bricks as shown in figure 5b.

### 3.1.7 Conclusion

Following conclusion can be drawn from the turbulent flow model.

- Turbulent flow of air from anode baking furnace can be implemented in COMSOL Multiphysics.
- Percentage flow of air in the middle part of section of furnace is lower and needs improvement.
- Tie-bricks induce higher turbulence thereby increasing mixing in the furnace.

## 3.2 Reacting turbulent flow

Modeling of reacting turbulent flow is complex as compared to above two models since it involves two physics, reaction and flow. In order to develop this model, several trial models were studied by changing geometry, initial and boundary conditions, mesh, numerical solver and study steps. Here, the most comparable model to the actual geometry and boundary conditions is explained.

### 3.2.1 Geometry

A simplified geometry as compared to that used in turbulent flow model is used for reacting turbulent flow modeling. Figure 6 shows the domain of the section from the furnace which is used as a geometry of this model. It depicts the small domain near the fuel inlet between two baffles.



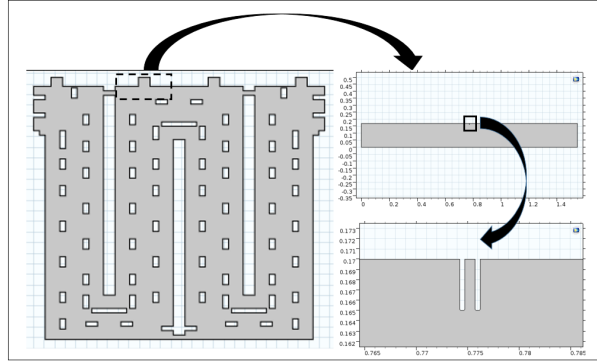
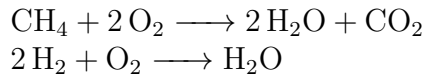


Figure 6: Geometry for the reacting turbulent flow model

As the fuel inlet is very small as compared to rest of the geometry, the fuel inlet is shown by enlarging some portion of the geometry. Dimensions of the geometry are such that the mass flow ratio of air to fuel from the actual furnace is reproduced. Trial models suggest that the variation in velocity (to adjust the mass flow ratio) affects the distribution of more than geometry. Therefore, velocity of fuel and air is in the same order as that in actual furnace but the dimensions are significantly different. Moreover, the current model is 2 dimensional as opposed to the actual 3 dimensional furnace which also justifies the use of different dimensions for air and fuel inlet.

### 3.2.2 Physics

In order to develop reacting flow model, "Chemical species transport" module with concentrated mixture type is chosen. Out of various models available in this module,  $k - \epsilon$  turbulent flow model is selected to describe turbulent viscosity and average kinetic energy parameters for RANS equations. Density of fluid is calculated by assuming gas as ideal gas and dynamic viscosity is taken as  $1 \times 10^{-5}$  Pa.s. Diffusion is described by Ficks's diffusion coefficient. Kays-Crawford mass transport turbulence model is used. Following 2 reactions are considered to occur in the entire domain of the geometry.



Rate constant is defined such that the reactions occur at infinitely fast rate. Therefore, system is turbulent mixing limited. This is a characteristic of non-premixed eddy dissipation model as described in section 2.4.3.

### 3.2.3 Boundary conditions

In this model, reactions are occurring in the turbulent flow of air in the furnace. This model solves turbulent flow equations such as continuity equation, RANS equation and equations of  $k-\epsilon$  model along with equations for mass transport and reaction rate equations. Therefore, required boundary conditions for velocity, pressure, average turbulent kinetic energy and turbulent dissipation rate remain same as that described in turbulent flow model 3.1.3. However, extra boundary conditions are required for chemical species (2 boundary conditions for each of the species). Table 3 presents the initial and boundary conditions for this model.

Table 3: Initial and boundary conditions

	Velocity ( $m/s$ )	Pressure ( $atm$ )	$k$ ( $m^2/s^2$ )	$\epsilon$ ( $m^2/s^3$ )	w_CH4	w_O2	w_CO2	w_H2O	w_H2	w_N2
Initial conditions	0	0	0	0	0.001	0.21	0.001	0.001	0.001	0.001
Inlet (air)	1.3	-	0.000254	0.006632	0.001	0.21	0.001	0.001	0.001	0.001
Inlet (fuel)	150	-	3.375	10188.08	0.905	0.006	0.002	0.003	0.001	0.083
Wall	0	-	wf	wf	wf	wf	wf	wf	wf	wf
Outlet	-	1	-	-	-	-	-	-	-	-

Last 6 columns give the weight fraction values for different chemical species. Figure 13 from the appendix A.3 represents the inlet for air, inlet for fuel, outlet and wall of the studied domain.

### 3.2.4 Mesh

In the present model, fine triangular mesh is used to divide the entire fluid domain into short sub-domains. Moreover, splitting function is used to handle sharp corners near the corner where fuel is introduced in the domain of air. With the use of splitting function, quadrilateral mesh can be obtained near the corners as shown in Figure 7.

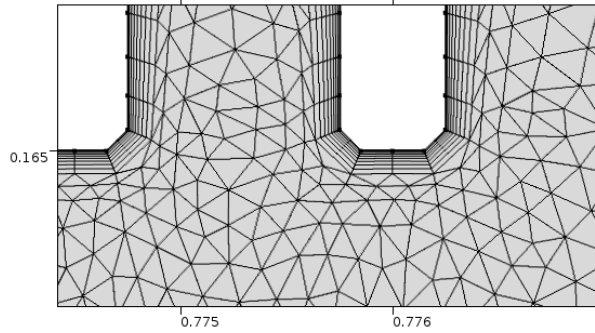


Figure 7: Mesh with splitting function for corner refinement from the reacting turbulent flow model

### 3.2.5 Study

Default linear discretization scheme is used to discretize the components of the equations. In order to solve the equations, PARDISO direct numerical solver is used. Segregated step approach is used to solve the different variables. Variables that are solved in different segregated steps are as shown in Table 4.

Table 4: Variables solved in segregated steps of reacting turbulent flow model

Study	Segregated step	Variables
Reacting turbulent flow	Step 1	Pressure Velocity
	Step 2	Turbulent kinetic energy Specific dissipation rate
	Step 3	Mass fraction of components

### 3.2.6 Results

Figure 8a represents the surface velocity plot in the studied domain with Figure 8b representing the enlarged fuel inlet.

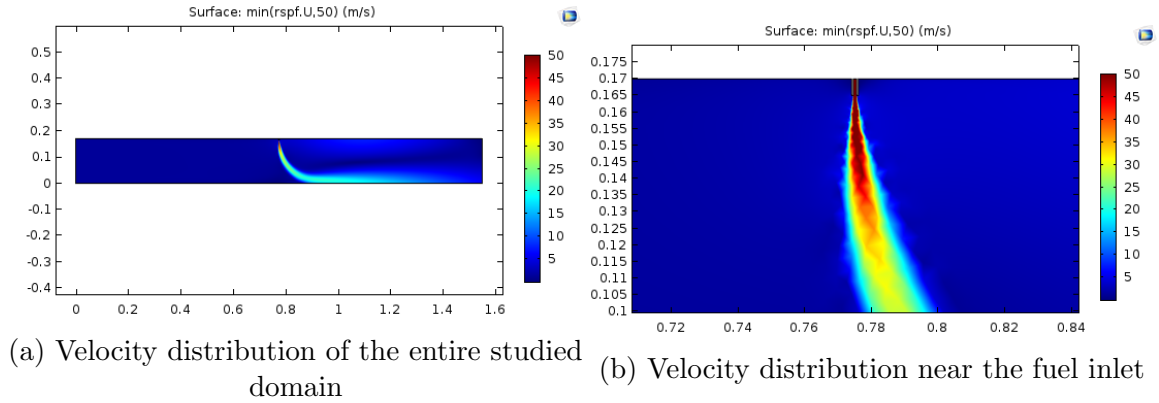


Figure 8: Model results of surface velocity of reacting turbulent flow

Velocity profile in the domain of reacting flow model suggests that the velocity is high in the small fuel domain, since the fuel is injected at very high velocity from the fuel inlet. As soon as it mixes with the air, velocity reduces and jet of fuel is deflected towards the outlet, due to air flow in that direction. This results align with the expected behaviour of velocity in the domain. Turbulence in the domain is observed

after the fuel is mixed with the air. This can be observed from the turbulent viscosity plot of Figure 15 of appendix B.2.

In the model, fuel mainly consists of  $\text{CH}_4$  which reacts with  $\text{O}_2$  from air. Therefore, mass fraction distribution of  $\text{CH}_4$  is as shown in Figure 9. Figure 10a shows that mass fraction of  $\text{CH}_4$  in the overall domain is not more than 10% though it is the major part of the injected fuel. The major mass fraction of  $\text{CH}_4$  is in the small tube through which fuel is injected (Figure 9b). As soon as  $\text{CH}_4$  mixes with air, it is reacted with  $\text{O}_2$  which reduces its mass fraction in the overall domain. This mass fraction decreases upto short distance after which it becomes constant in the direction of fluid flow. Due to mass flow ratio of  $\text{CH}_4$  to  $\text{O}_2$  and participation of  $\text{O}_2$  in another reaction, most of the  $\text{O}_2$  is consumed at the interface. Therefore, mass fraction of  $\text{CH}_4$  remains constant after short distance from the interface where air and fuel mixes.

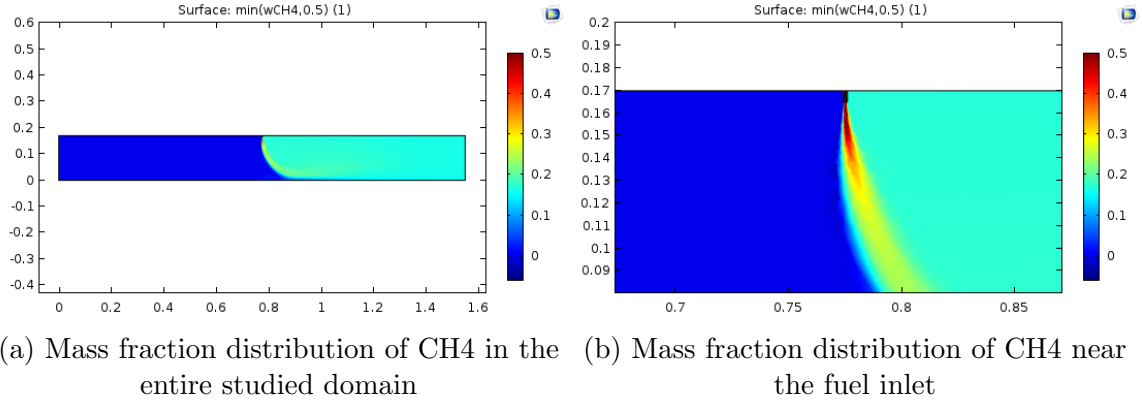


Figure 9: Model results of mass fraction distribution of  $\text{CH}_4$  in reacting turbulent flow

Mass fraction distribution of  $\text{CO}_2$  is as shown in Figure 10.

As can be expected,  $\text{CO}_2$  mass fraction in the left part, i.e., before the entry of fuel is negligible and it starts to appear after  $\text{CH}_4$  and  $\text{O}_2$  are mixed. Moreover, the  $\text{CO}_2$  concentration is highest at the interface suggesting that reaction occurs as soon as the two species are mixed. Mass fraction of  $\text{CO}_2$  becomes as most of the reaction occurs only at the interface where air and fuel mixes. Mass fraction distribution of other species also align with the expected behaviour of mass fraction in the domain.

### 3.2.7 Conclusion

With the reacting flow model, following conclusions can be drawn.

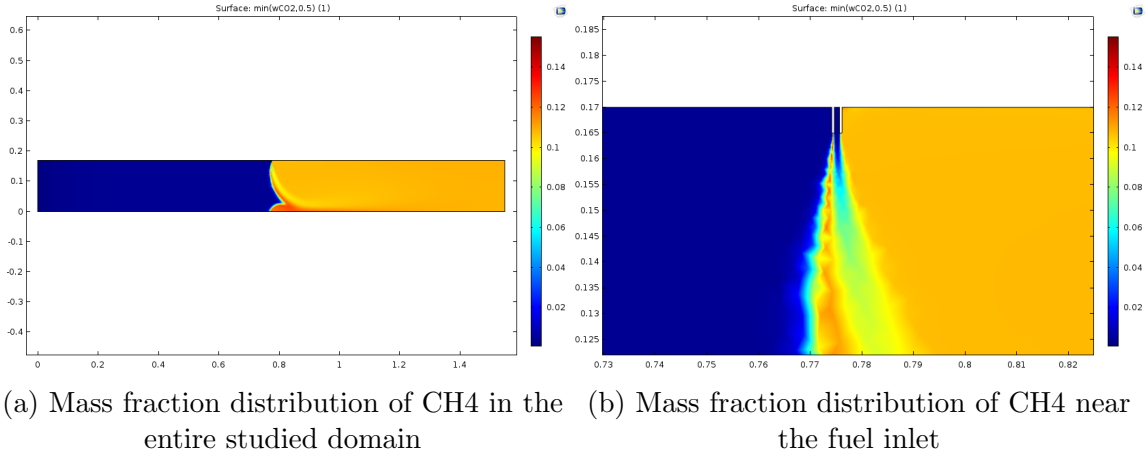


Figure 10: Model results of mass fraction distribution of CH4 in reacting turbulent flow

- Reacting turbulent flow of with desired mass flow ratio of air to fuel can be modeled using COMSOL Multiphysics
- Splitting function for the corner refinement of mesh helps in the better convergence
- Eddy-dissipation model can be implemented in COMSOL Multiphysics

### 3.3 Combined model of reacting flow and heat transfer

As a next step, heat effects were added to the reacting turbulent flow developed in section 3.2. In this model, heat flow through the gas by convection and radiation is included along with considering generation of heat through the combustion process. Conduction heat flow through the top wall is also considered in this model.

#### 3.3.1 Geometry

Geometry of this model is as shown in Figure 11. This geometry is similar to the reacting turbulent flow model but an extra top wall is added to account for the heat flow by conduction through the walls. The description of the fuel and air inlet and outlet is same as that of reacting turbulent flow model.

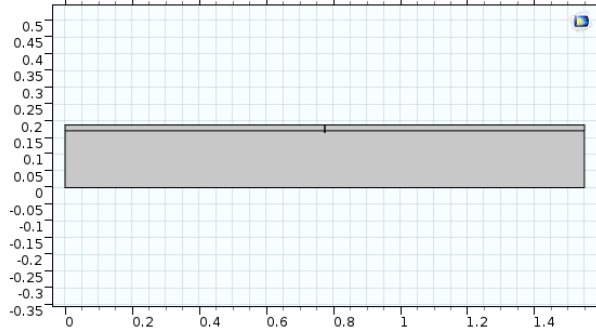


Figure 11: Geometry for the reacting turbulent flow model with added heat effects

### 3.3.2 Physics

In this model, along with the physics used in reacting flow model, heat transfer in fluids is also included from "Heat transfer" module of COMSOL Multiphysics. In order to deal with heat conduction through the top wall and radiation, two more settings, i.e., "heat transfer in solids" and "radiation in participating media" are also included.

Thermal diffusion coefficient of fluid is defined by equation 19.

$$k = k_{mix} + Cp_{mix} \times \frac{\mu_T}{0.72} \quad (19)$$

Here,  $k_{mix}$  is thermal conductivity of a mixture is equal to 0.1 W/(m.K) whereas, the third term is thermal conductivity induced by turbulence.  $Cp_{mix}$  is the heat capacity of mixture and  $\mu_T$  is the turbulence viscosity.  $Cp_{mix}$  is calculated by taking mole fraction weighted average of heat capacity of individual chemical species. Heat capacity (Cp) of individual species is assumed to be temperature dependent and is calculated by interpolation function. Cp of each species at three temperature is taken from the literature. Cp at a particular temperature is interpolated using these values. Heat conduction properties of wall as described as shown in Table 5.

Table 5: Heat conduction properties of wall

Property	Value	Unit
Density	2400	$kg/m^3$
Thermal conductivity	1.5	$W/(m * K)$
Heat capacity	18	$J/(Kg * K)$

Combustion products CO<sub>2</sub> and H<sub>2</sub>O participate significantly in radiative heat transfer. Therefore, Radiation in participating media is used to model radiation heat

transfer. P1 approximation method is used as a radiation discretization method. since, burning of natural gas can be treated as absorbing and emitting media, scattering coefficient is taken as 0. Absorption coefficient is extrapolated for a given furnace length using exponential function and using a data from the online forums [14]. This value turns out to be  $7 \text{ m}^{-1}$ .

### 3.3.3 Boundary conditions

This model also solves equations described in reacting turbulent flow. Therefore, boundary conditions for reacting turbulent flow are same as that used in section 3.2.3. However, extra boundary conditions are needed to describe heat addition implemented in this model. Heat effects can be divided into 3 major parts as following.

- Heat transfer in fluid by convection and conduction
- Heat transfer in solid by conduction
- Heat transfer in fluid by radiation

Boundary conditions for these parts described below.

For heat transfer in fluid by convection and conduction temperature at inlet of air and fuel are defined to be 293 K. In the fluid domain, heat is generated by the combustion process which is defined by following two equations.

$$dH_{R1} = (dH_{CO2} + 2 \times dH_{H2O}) - (dH_{CH4} + 2 \times dH_{O2}) \quad (20)$$

$$dH_{R2} = dH_{H2O} - (dH_{H2} + 0.5 \times dH_{O2}) \quad (21)$$

Here,  $dH_{R1}$  and  $dH_{R2}$  are enthalpy of generation by two reactions described in section 3.2.2. These enthalpies as can be seen from equation 20 and 21 are calculated based on the specific enthalpies of participating chemical species and their stoichiometric coefficient. The total heat generated in the fluid domain is calculated by equation 22.

$$dH = -(dH_{R1} \times Rate_{R1} + dH_{R2} \times Rate_{R2}) \quad (22)$$

Here,  $Rate_{R1}$  and  $Rate_{R2}$  are rate of reaction 1 and 2, respectively.

For heat conduction through the top wall, temperature of boundary which is in contact with external environment is defined to be 273 K. Whereas, temperature of the boundary in contact with fluid domain is defined as a variable temperature of fluid. For radiation through the fluid, Marshak boundary condition is used which is defined in appendix A.2. To define radiation intensity by this boundary condition, surface emissivities are needed. Inlet and outlet boundaries are assumed as black wall and

therefore surface emissivity for these boundaries is taken as 1. Whereas, other boundaries are considered as perfectly reflecting and therefore, surface emissivity for the wall is taken as 0.

### 3.3.4 Mesh

Mesh for this model is exactly same as that used in reacting flow model. Default fine triangular mesh is implemented for extra wall that has been added at the top.

### 3.3.5 Study

Default linear discretization scheme is used to discretize the components of the equations. In order to solve the equations, PARDISO direct numerical solver is used. Results of the reacting turbulent flow are used as the initial values for simultaneously solving two physics described in this model. A fully coupled approach is used to solve main variables which are temperature, mass fraction of different chemical species, velocity, pressure, turbulent kinetic energy and turbulent dissipation rate.

### 3.3.6 Results

Figure 12a represents the overall surface temperature distribution in fluid as well as solid domain.

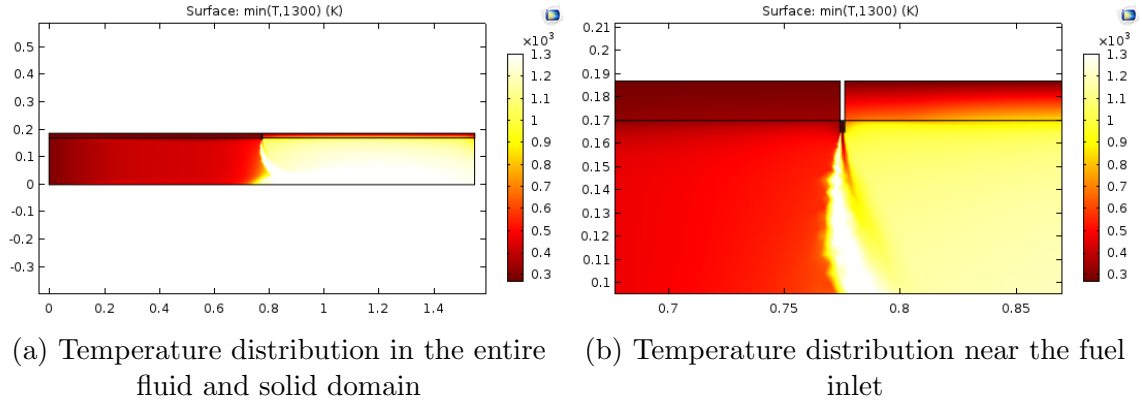


Figure 12: Model results of temperature of reacting turbulent flow with added heat effects

It can be observed from Figure 12a that the temperature in the overall region significantly varies after the interface, where fuel mixes with air. At the interface, combustion reaction occurs which generates large amount of heat, increasing the temperature at the interface. This temperature decreases till a short distance in the



fluid flow direction after which it becomes constant. As discussed in results section 3.2.6 of reacting turbulent flow model, most of the reaction occurs at the interface and upto a short distance from the interface in the direction of fluid flow. Therefore, the temperature distribution seen in Figure 12a aligns with these results.

Figure 12b shows the temperature distribution near the fuel inlet and through the top wall. Temperature of increases as soon as fuel mixes with air due to immediate occurrence of combustion reaction. Moreover, temperature distribution in the wall suggests steady decrease, confirming the conduction through the wall from higher temperature to lower temperature of the boundary in contact with the external environment.

### 3.3.7 Conclusion

Based on the temperature distribution results explain in the previous section, following conclusions can be drawn.

- Conjugate heat transfer can be implemented in reacting turbulent flow in COMSOL Multiphysics
- Radiation can be implemented in reacting turbulent flow in COMSOL Multiphysics
- Heat generation in the combustion process can be quantified in COMSOL Multiphysics

## 4 Further research

In the present work, a simplified model of combustion process in turbulent flow is developed in COMSOL Multiphysics. Generation of heat through combustion process, transfer of heat in fluid through radiation and heat conduction through the top wall are major heat effects added to the model. This model confirms that COMSOL Multiphysics can be used to implement physical models such as  $k-\epsilon$  turbulent flow model, eddy-dissipation model, P1 approximation model etc. In order to achieve the goal, i.e., to know the exact temperature distribution around the burner in anode baking furnace, following further research on the present model is required.

- In the present study, reacting turbulent flow is studied only in a small domain near the burner. Further research is needed considering the entire heating section of the furnace. This may require additional research into analysing different mesh types or numerical methods since convergence of the model of the entire section can be a problem.

- In the present work, only two major reactions are considered. However, to analyse NOx generation near the burner, addition of extra reactions such as formation of NOx are needed. This may require further research on modeling kinetic reactions.
- Radiation does not seem to affect temperature distribution in the present model as compared to the expected effect. Therefore, further research is needed on the absorbing coefficient, scattering coefficient of the walls. Moreover, further investigation using different radiation models can also be useful.
- Further research to extend this 2D model into 3D model is required since few components such as burner outlet is cylindrical in shape which can not be simply reproduced by linear extrusion in third direction. Using axis symmetric 2D model in order to solve this problem is also not possible as the rest of the geometry is not cylindrical.
- Present model is restricted to a physics in the flue walls of the furnace. However, further research is needed to model heat transfer through the walls between flue wall and pits as well as heat transfer through anode material.
- A combined model of flue wall along with the anode in the pit can be of importance as it would allow to incorporate release and burning of volatiles in the model.
- In this work, other important aspects such as air infiltration is not considered and can be incorporated in subsequent models.

## References

- [1] D. S. Severo, V. Gusberti, P. O. Sulger, F. Keller, and M. W. Meier, “Recent developments in anode baking furnace design,” in *Light Metals 2011*, pp. 853–858, Springer, 2011.
- [2] D. R. A. Fikri, “Modeling non-premixed turbulent combustion in industrial rotary kiln: Application in openfoam.” <http://repository.tudelft.nl/>, 2017.
- [3] H. K. Versteeg and W. Malalasekera, *An introduction to computational fluid dynamics: the finite volume method*. Pearson Education, 2007.
- [4] T. L. Bergman and F. P. Incropera, *Fundamentals of heat and mass transfer*. John Wiley & Sons, 2011.
- [5] Wikibooks, “Introduction to chemical engineering processes/atom balances — wikibooks, the free textbook project.” [https://en.wikibooks.org/w/index.php?title=Introduction to Chemical Engineering Processes/Atom balances&oldid=3132961](https://en.wikibooks.org/w/index.php?title=Introduction_to_Chemical_Engineering_Processes/Atom_balances&oldid=3132961), 2016.
- [6] D. Veynante and L. Vervisch, “Turbulent combustion modeling,” *Progress in energy and combustion science*, vol. 28, no. 3, pp. 193–266, 2002.
- [7] R. Borghi, “Turbulent combustion modelling,” *Progress in Energy and Combustion Science*, vol. 14, no. 4, pp. 245–292, 1988.
- [8] N. Peters, *Turbulent combustion*. Cambridge university press, 2000.
- [9] B. F. Magnussen, “The eddy dissipation concept: a bridge between science and technology,” in *ECCOMAS thematic conference on computational combustion*, pp. 21–24, 2005.
- [10] H. Pitsch, “Turbulent non-premixed combustion,” *CEFRS Combustion Summer School*, 2014.
- [11] L. A. Dombrovsky and D. Baillis, *Thermal radiation in disperse systems: an engineering approach*. Begell House New York, 2010.
- [12] C. Ansys, “Release 11.0,” *ANSYS CFX-solver theory guide*, ANSYS, 2006.
- [13] F. Göbel and C. Mundt, “Implementation of the p1 radiation model in the cfd solver nsmb and investigation of radiative heat transfer in the same main combustion chamber,” in *Proc. 17th AIAA Int. Space Planes and Hypersonic Systems and Technologies Conference*, 2011.

- [14] CFD, “Cfd online.” <https://www.cfd-online.com/Forums/main/2112-scattering-coefficient-1-m.html>, Scattering coefficient, May 2000.

## A Boundary conditions

### A.1 Wall function

Wall function boundary condition is used to incorporate the changing behaviour of flow from wall to the domain away from the wall. Following integrated equations define the wall function boundary condition for velocity, average turbulent kinetic energy and turbulent dissipation rate.

$$u \cdot n = u_s \quad (23)$$

$$\rho u_s = \sum n \cdot N_{i,tot} \quad (24)$$

$$[(\mu + \mu_T)(\nabla u + (\nabla u)^T) - \frac{2}{3}(\mu + \mu_T)(\nabla \cdot u)I - \frac{2}{3}\rho k I]n = -\rho \frac{u_\tau}{\delta_w^+} u_{tang} \quad (25)$$

$$u_{tang} = u - (u \cdot n)n \quad (26)$$

$$\nabla k \cdot n = 0 \quad (27)$$

$$\epsilon = \rho \frac{C_\mu k^2}{\kappa_v \delta_w^+ \mu} \quad (28)$$

### A.2 Marshak boundary condition

According to the Marshak boundary condition radiation intensity at the wall is defined by the following equation.

$$q_w = -\frac{1}{3\kappa_\lambda} n \cdot \nabla G = -\frac{\epsilon_w}{2(2 - \epsilon_w)} (4\sigma T_w^4 - G_w) \quad (29)$$

### A.3 Boundary conditions for reacting turbulent flow

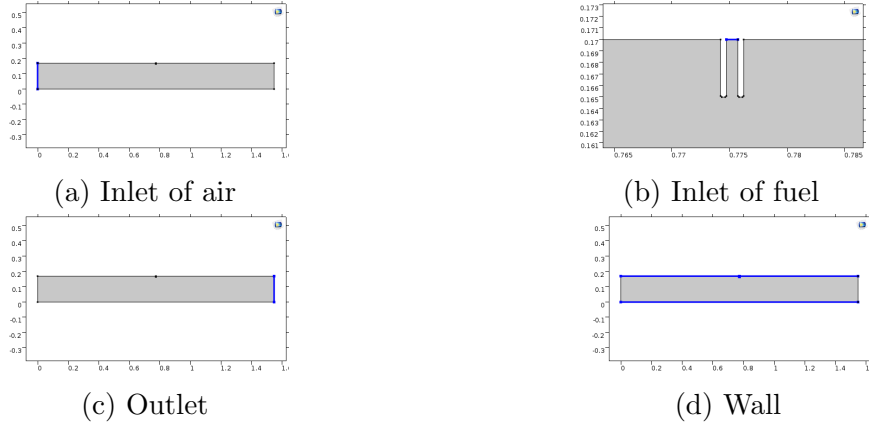


Figure 13: Boundary conditions of reacting turbulent flow model

## B Results

### B.1 Turbulent flow model

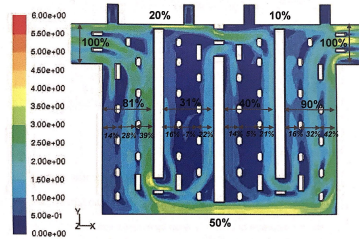


Figure 14: Previously studied turbulent flow model by RioTinto Alcan

### B.2 Reacting turbulent flow model

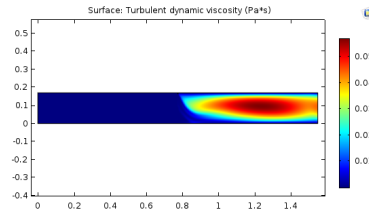


Figure 15: Turbulent viscosity in reacting turbulent flow

Copyright © 2010 by Delft Institute of Applied Mathematics, Delft, The Netherlands.

No part of the Journal may be reproduced, stored in a retrieval system, or transmitted, in any form or by any means, electronic, mechanical, photocopying, recording, or otherwise, without the prior written permission from Delft Institute of Applied Mathematics, Delft University of Technology, The Netherlands.